Ibn Al-Haitham Journal for Pure and Applied Sciences
Journal homepage: jih.uobaghdad.edu.iq
PISSN: 1609-4042, EISSN: 2521-3407
IHJPAS. 2025, 38(3)

Impact of Annealing on Optical and Structural Analysis of Chemically Spray-Prepared Nickel Oxide Thin Films

Shatha. F. Abbas[1*] and Hiba M. Ali[2]
[1,2] Department of Physics, College of Education for Pure Sciences (Ibn Al-Haitham), University of Baghdad, Baghdad, Iraq.
*Corresponding Author.

Received: 16 December 2024 Accepted: 23 April 2025 Published: 20 July 2025
doi.org/10.30526/38.3.4073

Abstract

In this study, we prepared thin films of nickel oxide with a thickness of 150±10 nm using the pyrolysis spray technique, and their properties were studied for two hours at different annealing temperatures. including (as deposited, 723 and 873) K. Based on XRD measurements, the pattern data showed that (NiO) had an amorphous structure without annealing, but that a cubic polycrystalline structure with a preferred orientation (111), (200), and (220) was produced at a higher annealing temperature. In addition to other techniques, the crystal structure of the film was characterized using X-ray diffraction. The structure and physical characteristics of the NiO thin films are examined using methods based on atomic force microscopy and X-rays. techniques are employed to examine the surface morphology of layers of nickel oxide. As the temperature of annealing increased, the study reported mean diameter, roughness of surface, and particle size mutation values (186.0–254 nm). The wavelength range of (300-1000) nm is also taken into consideration when further examining and reporting transmittance and absorbance spectra, demonstrating various deviations from the nominal values. The results show that a treatment of temperature 873 K produced the sample's maximum absorbance value. The findings indicate that direct transitions are allowed in the thin films under study at optical energies of (3.57, 3.51, and 3.47) eV, respectively.

Keywords: Nickel oxide, Annealed temperature, X-ray diffraction, Characteristic optical.

1. Introduction

The nickel oxide is an important p-type antiferromagnetic semiconductor with exceptional electrochemical, catalytic, and gas-sensing capabilities. Its application in solid-state sensors, electrochromic devices, lithium batteries, and heterogeneous catalysts has been thoroughly studied (1-3). Several techniques were used to create the nickel oxide thin films, such as Chemically Spray-Prepared. The development of hybrid NiO with copper nanoparticles could be used for the fabrication of thin films for enhanced optoelectronic devices (3, 4). NiO is known for its favorable characteristics, such as a high level of optical transmission and p-type

semiconductor properties. For producing superior nickel oxide thin films with homogenously dispersed copper nanoparticles. The optical characteristics of thin films may be actively controlled using a variety of manufacturing techniques (5-7). The findings also demonstrate that pyrolysis procedures combined with thermal annealing can produce nickel oxide coatings that are more uniform and crystallinity-enhancing., which are preferred for obtaining the required properties enhance the electron transport properties and thus enhances the overall photovoltaic efficiency of the solar cells when compared to solar cells prepared with pure NiO films (8-10). Additionally, the changes in deposition parameters such as temperature and concentration of the precursors have a profound impact on the optical properties, resulting in higher transmittance values as well as reduced band gap energy (11-13).

2. Materials and Methods

Making Thin Film NiO thin films was made using a solution of nickel nitrate hexahydrate [Ni(NO3)2, 6H,0]. A few drops of nitric acid (HNO_3) were added as a stabilizer after the precursor had been dissolved in double-distilled water. Additionally, the mixture is agitated for 45 minutes at room temperature using a magnetic stirrer until it becomes translucent and clear (14-16).

$$M = \frac{mt}{Mwt} \times \frac{1000}{V} \quad (1)$$

In this case, M is molecular concentration, Mt is for material weight, Mwt is for molecular weight, and V is for volume. As substrates, microscopic glass slides measuring 75 × 25 x 1.1 mm' were employed. After being washed with distilled water and alcohol in an ultrasonic bath, they were blow-dried using dry air (17–19). Nickel oxide coatings with a thickness of 150 nm and a vertical distance of 24 cm between the sprayer's tip and the substrates were produced by heating the substrates to 400°C and placing them on a rotating base at medium speed and a spray rate of 0.16 ml/sec in pressure (10^5) N /m^^{2}. The films were allowed to cool to room temperature following deposition. Following deposition, the film was annealed for two hours at two different temperatures (723 and 873) K. We examined the surface morphological properties of the film using atomic force spectroscopy (AFM). With wavelengths spanning from 300 to 1000 nm, we used a UV-Vis spectrophotometer to get the transmittance and absorbance spectra at normal incidence. After the coated materials' spectra were analyzed, the energy gap was calculated using the Tauc equation. The technique of atomic force microscopy was used for evaluating the surface morphologies of the materials.

3. Results and Discussion

3.1. Structural Analysis

3.1.1. XRD Analysis

Figure (1) shows the outcomes of two higher temperatures annealing of NiO thin films made on glass substrates (from 723 to 873 K as-deposited). Metaphors and similes polycrystalline cubic phases are present in all thin films, and the XRD pattern of a NiO sample has a prominent peak at [(111), (200), and (220)], Found on the card (ICCD 00-04-0835), the 2 theta angle ranged from 20 to 80 deg. It appears that raising the annealing temperature enhances the thin films' crystallinity. The classic Scherrer's Equation, which is used to determine the Crystalline size of NiO thin films, is given in **Table1** (**15** and **16**). Crystalline size (C.S) may be calculated using Scherrer's Equation (17).

$$C.S = \frac{0.94\lambda}{\beta \cos \theta} \quad (2)$$

The symbols for Bragg's angle (θ), the X-ray wavelength of 1.54056 (λ), and the full width half maximum of the primary peak (FWHM) were used.

Table 1. Diffraction of X-ray NiO during various annealing temperatures (as-deposited,723, and 873) K

T_a (K)	2 Θ_{exp}	2 Θ ASTM	FWHM (deg)	d_{exp} (Å)	d (A) ASTM	Planes (hkl)	C.S (nm)
	37.304	37.279	0.5156	2.407	2.410	111	**16.97**
723	44.333	43.295	0.4130	2.083	2.088	200	**21.68**
	63.134	62.913	0.4314	1.473	1.476	220	**22.56**
	37.385	37.279	0.4228	2.403	2.410	111	**20.71**
873	43.297	43.295	0.3220	2.081	2.088	200	**27.71**
	62.318	62.913	0.3439	1.473	1.476	220	**28.18**

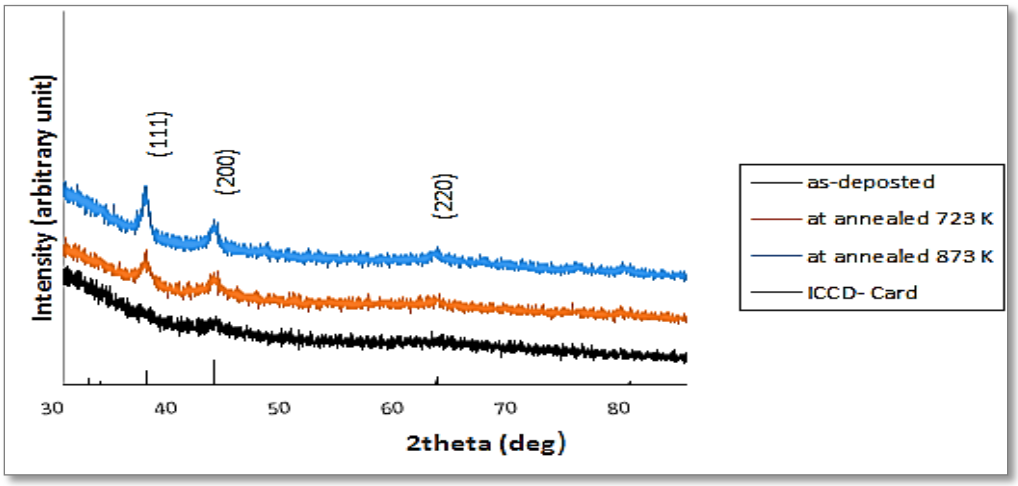

Figure 1. NiO thin-film XRD-diffraction patterns (as-deposited, 723, and 873) K with varying annealing temperatures

3.1.2. The Analysis of Surface Morphology

Figure (2) demonstrates that no new peak was observed during Annealing at a temperature, and the significant enhancement of the crystal structure was eliminated. Additionally, when Ta rises, the crystallite size increases. According to earlier research, it is evident that higher annealing temperatures cause the films to crystallize more (19, 20). The films' particle sizes grow as the annealing temperature rises. Although the surface was continuously smooth, we discovered that the RMS value fluctuated. Annealing only marginally enhances surface roughness. The structure grew clearer, and some deep troughs formed. Smooth surfaces and nano-scale particles are present in films made and annealed at (723 and 873) K.

Table 2. AFM parameters (Average Diameter, Roughness average and RMS roughness) for NiO samples (As-deposited, 723and 873) °K.

T(K)	Average diameter (nm)	roughness Surface (nm)	RMS (nm)
As-deposited	186.0	10.08	6.928
723	157.0	12.56	7.668
873	254.0	18.25	9.458

Table (2) lists in Average diameter, roughness surface, (RMS) values, and surface Average grain size are listed in **Table (2**). It can be noticed that these values rose as the annealing temperature (723 and 873) °K increased due to the NiO films' crystallization brought on by thermal annealing. Grain recrystallization may occur when the temperature rises (21, 22).

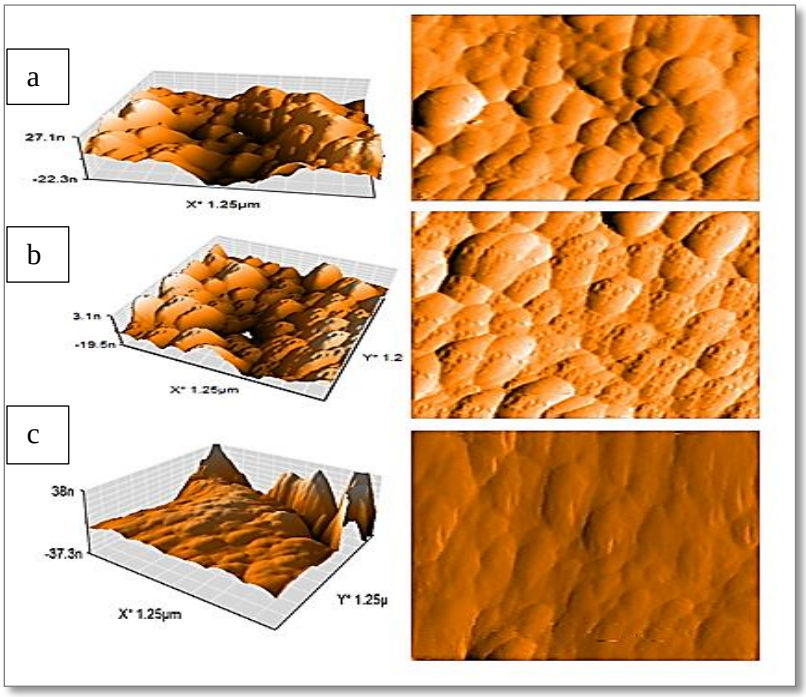

Figure 2. Images of NiO in two dimensions and three dimensions between two distinct annealing temperatures ((a) As deposited, (b) 723, and (c) 873) °K.

3.2. Optical Analysis

Figure 3 displays the NiO films' optical transmittance spectrum. All thin films with high visible-range transmittance have low oxygen ion vacancy concentrations. (23). The transmittance measurements show a sharp decline below λ = 300 nm, suggesting substantial band-to-band absorption (24). Raising the annealing temperature led the absorption edges to shift to lower energy ranges, which reduced the band gaps but had no discernible effect on the films' overall transmittance.

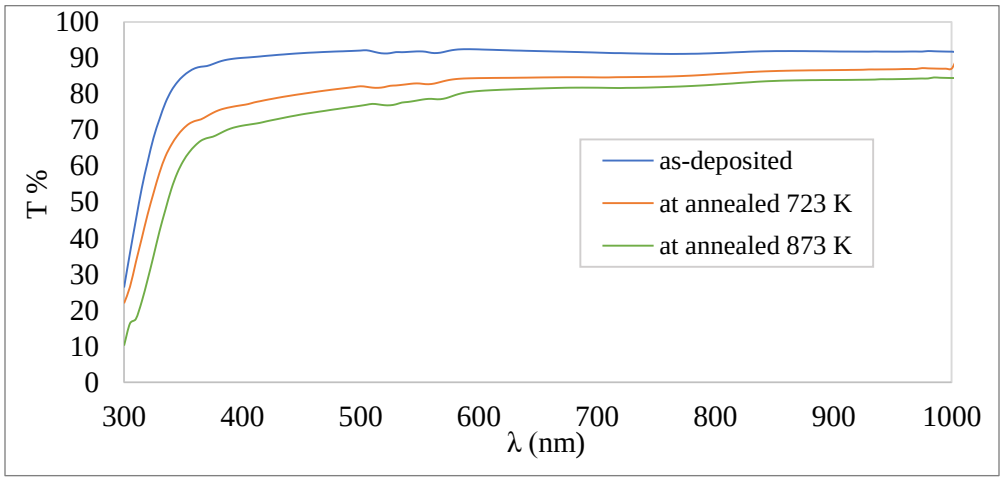

Figure 3. Shows the wavelength-dependent transmission spectrum for NiO films.

The absorption coefficient is a measurement of a material's capacity to absorb light. The absorption rate is significantly influenced by the band gap and photon energy. **Figure (4)** shows the impact of photon energy on the coefficient of optical absorption (α) for the NiO films for annealing. Considering the equations (25-30), which may be expressed

$$\alpha = (2.303)(A)/(t) \quad (3)$$

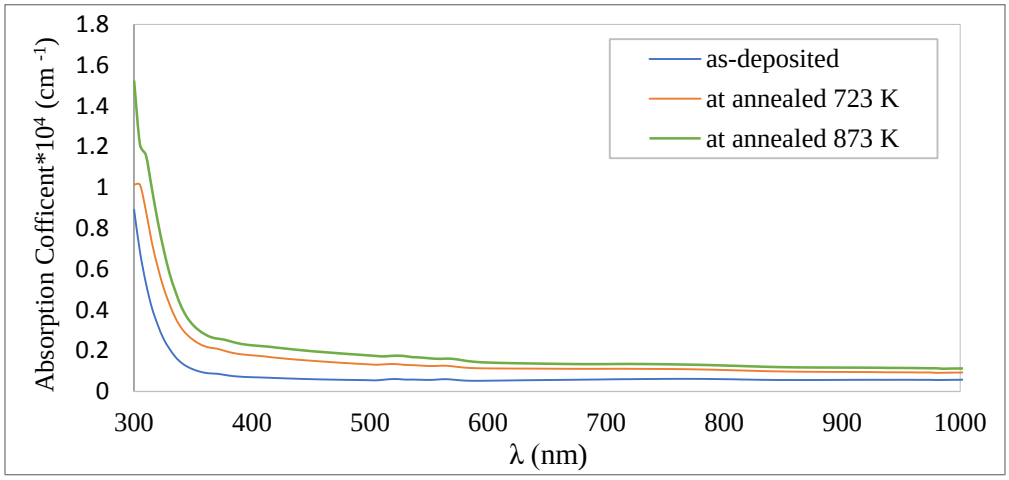

Figure 4. The absorbing coefficient of NiO particle thin films as a function of wavelength at two annealing temperatures

Figure (5) displays the plotted graphs of $(\alpha h \nu)^2$ eV. At two temperatures of 723 and 873 °K, the optical energy gaps of the resultant NiO thin films were determined to be 3.52, 3.41, and 3.23 eV, respectively. This is corroborated by the fact that, in addition to its effect on flaws, the annealing process changes the atoms' internal structure. These flaws would manifest as both shallow and deep levels in the complex semiconductor material's band gap. According to previous studies (15–19), the temperature-induced increase in grain size generated a shift in the band gap of annealed films (31-33).

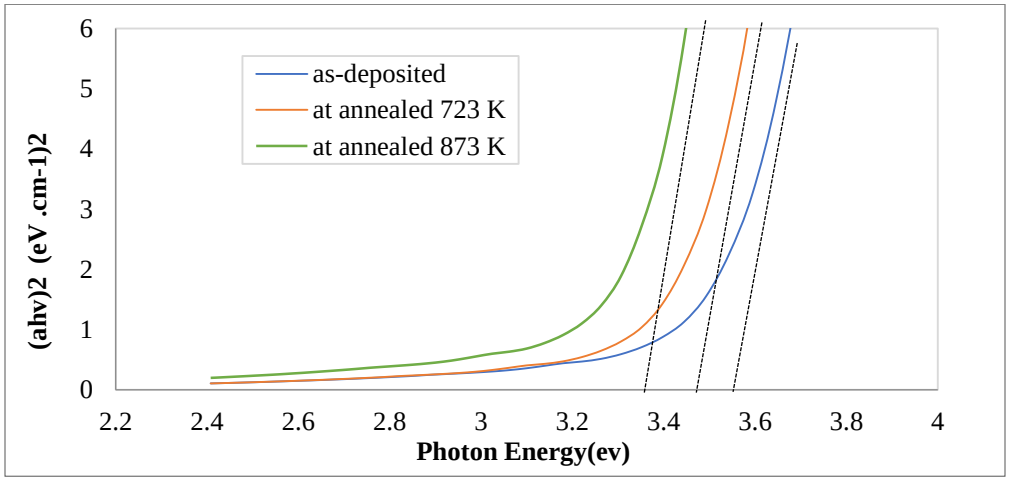

Figure 5. NiO films' (hv) photon energy at (As-deposited, 723and 873) °K are annealed at Two temperatures.

4. Conclusion

Chemical pyrolysis by spraying was used to deposit nickel oxide thin films. Two annealing temperatures were used for evaluating the properties of these films. Columnar growth enhances the optical and structural properties of the 873K annealed films, making them useful in photodetector applications. The XRD patterns showed that all of the deposited components had a cubic structure. The mean diameter size grew from 186 to 254 nm with a two-degree increase in annealing temperature. Nano-crystalline thin film production is encouraged by the annealing temperature. The energy band gap is 3.57, 3.51, and 3.47 eV before and after annealing, respectively.

Acknowledgment

I would like to thank the staff of the Physics Department, Deanship of the College of Education for Pure Science (Ibn Al-Haitham) for their support in writing this research.

Conflict of Interest

The authors declare that they have no conflicts of interest.

Funding

None.

Ethical Clearance

The project was approved by the local ethical committee at the University of Baghdad.

References

1. Thota S, Shim JH, Sera MS. Size-dependent shifts of the Neel temperature and optical band-gap in Nio nanoparticles. J Appl Phys.2013;114(21):214307. https://doi.org/10.1063/1.4838915.
2. Mustafa MH, Shihab AA. Influence of heat treatment on the efficiency of WO3: AuNPsoptoelectronic device prepared by spray pyrolysis technique.Theor App/ Phys. 2024;11:224. https://doi.org/10.57647/j.tap.2024.si-AICIS23.07.
3. Sasi B, Gopchandran K, Manoj P, KoshyP, Rao P, Vaidyan VK. Preparation of transparent and semi-conducting NiO films. Vacuum. 2003;68(2):149-154. https://doi.org/10.1016/S0042-207X(02)00299-3.
4. Miao HJ, Piron DL. Electro deposition of Ni-transition alloys for the oxygen evolution reaction. J Appl Electrochem.1991;21:55-9. https://doi.org/ 10.1007/BF01103830.
5. Varunkumar K, Hussain R, Hegde G, Ethiraj AS. Effect of calcination temperature on Cu-doped NiO nanoparticles prepared via wet chemical method: Structural, optical and orphological studies. Mater Sci Semicond Process. 2016;66:149-156. https://doi.org/10.1016/j.mssp.2017.04.009.
6. Begum ME, Chowdhury MNA, Islam MB. Structural, morphological, and optical characterizations of spray-pyrolyzed nickel oxide thin films. Results Mater.2022;14:100265. https://doi.org/10.1016/j.rinma.2022.100265.
7. Hussein BH, Khudayer HI, Mustafa MH,Shaban HA. Effect of V, In, and Cu doping on properties of p-type ZnSe/Si heterojunction solar cell. An Int J.2019;13(2):173. https://doi.org/ 10.1504/PIE.2019.099358.
8. Haichour A, Hamdaoui NE. Effects of copper doping and annealing temperature on the structural, morphological and optical properties of Nio thin films. J Nano Electron Phys.2019;11(6):06020. https://doi.org/10.21272/ jnep. 11(6).06020.

9. Patti V, Pawar S, Chougule M, Godse P, Sakhare R, Sen S. Effect of annealing on structural, morphological, electrical, and optical studies of nickel oxide thin films.J Surf Eng Mater Adv Technol. 2011;1 (1):35-41. https://doi.org/10.4236/ jsemat.2011.12006.
10. Abdel-wahab M, El Emam H, El RoubyWK. Sputtered Cu-doped NiO thin films as an efficient electrocatalyst for methanol oxidation. RSC Adv.2023;13 (18):10829-35. https://doi.org/10.1039/ d3ra00380a.
11. Tarea HS. Study the effect of rapid thermal annealing on thin films prepared by pulse laser deposition method. Eng Tech J. 2014;32(B):3-4.
12. Ali LS, Shehab AA, Abd AN. Preparation and characterization of p-NiO: Li thin films as Schottky photodiode. J Phys Conf Ser. 2019;1234:012013. https://doi.org/10.1088/1742-6596/1234/1/012013.
13. Ali HM, Khudayer JH. Influence of annealing on the physical properties of silver selenide thin film at different temperatures by thermal evaporation.Ibn Al-Haitham J Pure Appl Sci. 2023;36(2):147-155. https://doi.org/10.30526/36.2.2990.
14. Iman HK, Bushra HH, Mohammed HM, Ayser J. Investigation of the structural, optical, and electrical properties of AglnSe2 thin films. Ibn Al-Haitham J Pure App/ Sci. 2018;31. https://doi.org/10.30526/31.1.1848.
15. Bertus LM, Enesca A, Duta A. Influence of spray pyrolysis deposition parameters on the optoelectronic properties of WO3 thin films. Thin Solid Films. 2012;520(13):4282-4290. https://doi.org/10.1016/ j.tsf.2012.02.058.
16. Mustafa MH, Shihab AA. Effect of ratio gold nanoparticles on the properties and efficiency photovoltaic of thin films of amorphous tungsten trioxide. J Ovonic Res. 2023;19(6):23-34. https://doi.org/10.15251/JOR.2023.196.623.
17. Ukoba KO, Eloka-Eboka AC, Inambao FL.Review of nanostructured NiO thin film deposition using the spray pyrolysis technique. Energy Rev. 2018;82:2900-15. https://doi.org/10.1016/j.rser.2017.10.041.
18. Al-Sehemi AG, Al-Shihri AS, Kalam A,Dud GT, Ahmad T. Microwave synthesis, optical properties, and surface area studies of NiO nanoparticles. J Mol Struct. 2014;1058(1):56-61. https://doi.org/10.1016/ j.molstruc.2013.10.065.
19. Khodair ZT, Al-Jubbori MA, Shano AM,Sharrad Fl. Study of optical and structural properties of (NiO) 1-x(CuO)x nanostructures thin films. Chem Data Collect. 2020;100414. Bb https://doi.org/ 10.1016/ J.cdc.2020.100414.
20. Mustafa MH, Shihab AA. The effect of annealing process on surface plasmon resonances in tungsten trioxide films. Ibn Al-Haitham Pure App/ Sci.2024;37:44. https://doi.org/10.30526/37.4.3627
21. Goel R, Jha R, Ravikant C. Investigating the structural, electrochemical, and optical properties of p-type spherical nickel oxide (NiO) nanoparticles. J Phys Chem Solids. 2020;144:109488. https://doi.org/ 10.1016/j.jpcs.2020.109488.
22. Meenakshi LJ, Aswathy BR, Manoj PK.Effect of annealing temperature on structural and optical properties of nickel oxide thin films by dip coating method. AlP Conf Proc. 2020;2287(1):020007. https://doi.org/10.1063/5.0029961.
23. Godse P, Sakhare R, Pawar S, ChouguleM, Sen S, Joshi P, et al. Effect of annealing on structural, morphological, electrical and optical studies of nickel oxide thin films. J Surf Eng Mater Adv Technol. 2011;1(2):35. https://doi.org/10.4236/ jsemat.2011.12006.
24. Goel R, Jha R, Ravikant C. Investigating the structural, electrochemical, and optical properties of p-type spherical nickel oxide (NiO) nanoparticles. J Phys Chem Solids. 2020;144:109488. https://doi.org/10.1016/j.jpcs.2020.109488
25. Meenakshi LJ, Aswathy BR, Manoj PK. Effect of annealing temperature on structural and optical properties of nickel oxide thin films by dip coating method. AIP Conf Proc. 2020;2287(1):020007. https://doi.org/10.1063/5.0029961

26. Godse P, Sakhare R, Pawar S, Chougule M, Sen S, Joshi P, et al. Effect of annealing on structural, morphological, electrical, and optical studies of nickel oxide thin films. J Surf Eng Mater Adv Technol. 2011;1(02):35. https://doi.org/10.4236/jsemat.2011.12006
27. 2Sriram S, Thayumanavan A. Structural, optical, and electrical properties of NiO thin films prepared by low-cost spray pyrolysis technique. Int J Mater Sci Eng. 2014;2(2):118–121. https://doi.org/10.12720/ijmse.1.2.118-121
28. Joraid A, Alamri SN. Effect of annealing on structural and optical properties of WO3 thin films prepared by electron-beam coating. Phys B Condens Matter. 2007;391(2):199–205. https://doi.org/10.1016/j.physb.2006.09.010
29. Ali SM, Hassun HK, Salih AA, Athabb RH, Al-Maiyaly BK, Hussein BH. Study the properties of Cu2Se thin films for optoelectronic applications. Chalcogenide Lett. 2022;19(10):663–71. https://doi.org/10.15251/CL.2022.1910.663
30. Han D, Otani Y, Noda Y, Onishi T, Majima M, Uda T. Strategy to improve phase compatibility between proton conductive $BaZr_{0.8}Y_{0.2}O_3$-δ and nickel oxide. RSC Adv. 2016;6(23):19288–19297. https://doi.org/doi:10.1039/C5RA26947D.
31. Yadav AA, Chavan UJ. Influence of substrate temperature on electrochemical supercapacitive performance of spray deposited nickel oxide thin films. J Electroanal Chem. 2016 Dec;782:36–42. https://doi.org/10.1016/j.jelechem.2016.10.006.
32. Athab RH, Hussein BH. Fabrication and study of characteristics of HgSr2Can-1CunOδ+10 (n = 1, 2, and 3) thin films superconducting. Digest J Nanomater Biostruct. 2022;17(4):1173–1180. https://doi.org/10.15251/DJNB.2022.174.1173.
33. Bushra HH, Hanan KH. Study and preparation of optoelectronic properties of AgAl1-xInxSe2/Si heterojunction solar cell applications. NeuroQuantology. 2020;18(5):77–87. https://doi.org/10.14704/nq.2020.18.5.NQ20171